

## Article

# Differential Expression of miRNAs and Their Predicted Target Pathways in Cochlear Nucleus Following Chronic Noise Exposure in Rats

Chang Ho Lee, Jiwon Jeon, So Min Lee and So Young Kim \*

Department of Otorhinolaryngology-Head & Neck Surgery, College of Medicine, CHA University, Seongnam 13496, Korea; hearwell@gmail.com (C.H.L.); tw7682@nate.com (J.J.); lws6812@naver.com (S.M.L.)

\* Correspondence: sossi81@hanmail.net; Tel.: +82-31-780-5340

**Abstract:** Several recent preclinical studies have reported that dynamic changes in miRNA expression contribute to hearing function. This study aims to investigate miRNA expression changes in the cochlear nuclei (CN) of rats following chronic noise exposure. Eight-week-old rats ( $n = 14$ ) were exposed to noise for 4 weeks. The control rats ( $n = 14$ ) were raised under identical conditions without noise. Two months after noise exposure, the auditory brainstem response (ABR) was examined, and the cochlea and CN were harvested. In the CN, the expression levels of arc, neurocan, and brevicin were measured ( $n = 6$  per group). Furthermore, the expression levels of miRNAs and their predicted target genes were measured in the CN ( $n = 8$  per group). ABR thresholds were elevated after 4 weeks of noise exposure, which were maintained for 3 months. In CN, the protein expression of arc and brevicin was higher in the noise-exposed group than in the control group (0.95 [standard deviation (SD) = 0.53] vs. 3.19 [SD = 1.00],  $p < 0.001$  for arc and 1.02 [SD = 0.10] vs. 1.66 [SD = 0.24],  $p < 0.001$  for brevicin). The noise-exposed rats exhibited lower expression levels of miR-758-5p, miR-15b-5p, miR-212-3p, miR-199a-5p, and miR-134-3p than the control rats (all  $p < 0.001$ ). The AMPK signaling pathway was predicted to be regulated by these miRNAs. The predicted target genes AKT3, SIRT1, and PRKAA1 were highly expressed in noise-exposed rats. In CN of noise-exposed rats, the miRNAs of miR-758-5p, miR-15b-5p, miR-212-3p, miR-199a-5p, and miR-134-3p were reduced and related to AMPK signaling including AKT3 and SIRT1 expression. These modulation of signaling pathways could mediate the increased expression of brevicin in the CN of noise-exposed rats.

**Keywords:** microRNAs; noise; hearing loss; cochlear nucleus; AKT3; SIRT1



**Citation:** Lee, C.H.; Jeon, J.; Lee, S.M.; Kim, S.Y. Differential Expression of miRNAs and Their Predicted Target Pathways in Cochlear Nucleus Following Chronic Noise Exposure in Rats. *Cells* **2022**, *11*, 2266. <https://doi.org/10.3390/cells11152266>

Academic Editor: Daniele Nosi

Received: 26 May 2022

Accepted: 20 July 2022

Published: 22 July 2022

**Publisher's Note:** MDPI stays neutral with regard to jurisdictional claims in published maps and institutional affiliations.



**Copyright:** © 2022 by the authors. Licensee MDPI, Basel, Switzerland. This article is an open access article distributed under the terms and conditions of the Creative Commons Attribution (CC BY) license (<https://creativecommons.org/licenses/by/4.0/>).

## 1. Introduction

The cochlear nucleus (CN) is an important auditory brainstem that controls auditory perception and synaptic plasticity following external stimuli such as noise exposure [1]. The evolutionary auditory hindbrain, including the CN, represents therman-specific features of the auditory nervous system, which may contribute to the high-frequency hearing ability (>15–20 kHz) [2]. The restriction of synaptic plasticity and maintenance of high-frequency synaptic relays have been reported to be linked with high density of perineuronal nets (PNs) in the CN [3]. The chondroitin sulfate proteoglycans (CSPGs), such as brevicans and neurocans, are composed of PNs [4]. Changes in the PNs following noise exposure have been reported in the primary auditory cortex [5,6]. However, the changes in PNs or CSPGs have not been explored in the auditory brainstem of noise-induced hearing loss model.

As short non-coding transcripts, miRNAs orchestrate the transcription or translation of genes during development and pathological conditions, including auditory deprivation [7,8]. As miRNAs are abundant in the central nervous system and harbor multiple target genes, they are thought to regulate the neural pathways of neurogenesis and synaptogenesis [9,10]. For instance, miRNAs may suppress the translation of synaptic mRNAs before exposure to external stimuli such as chronic stress, which can induce synaptic plasticity [11].

Several recent preclinical studies have reported that dynamic changes in miRNA expression contribute to hearing function [7,8,12,13]. miRNAs are presumed to regulate the development of hearing function [7]. Among the 12 abundant miRNAs in the cochlea, 9 show dynamic changes during developmental periods and 11 are differentially expressed in the CN and superior olivary complex of the auditory hind brain [7]. Noise exposure has been suggested to alter miRNA expression in the CN [8]. Even as short as 2 h of noise exposure could induce changes in miRNA expression in the CN, although hearing thresholds were recovered [8]. However, changes in miRNA expression following chronic noise exposure have not been investigated.

Previous studies demonstrated the changes of CSPGs including brevican in auditory nervous system following noise-induced hearing loss [5,6]. The mediating role of miRNAs were suggested for the changes of CSPGs in visual cortex [14]. Therefore, we hypothesized that chronic noise exposure might induce changes in the expression of miRNAs that mediate synaptic plasticity, such as change of CSPGs, in the CN. To test this hypothesis, adult rats were exposed to chronic noise, and miRNA levels were examined. The target genes and signaling pathways for the dysregulated miRNAs were predicted, and the expression levels of CSPGs, neurocan, and brevican were estimated in the CN of noise-exposed rats.

## 2. Results

The noise was periodically exposed for 4 weeks in the noise-exposed rats (Figure 1). The hearing levels were measured at 1 week, 2 weeks, 2 months, and 3 months after the noise exposure.

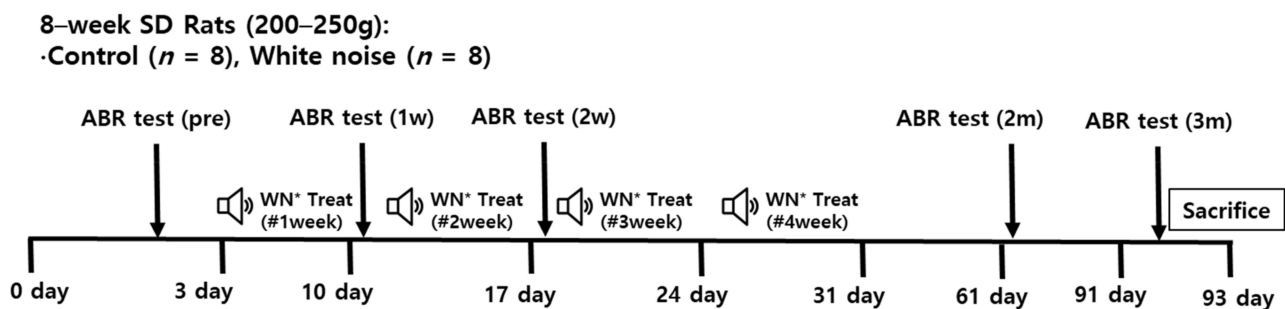


**Figure 1.** Design of the present study ( $n = 8$  per group). Noise was experienced by the rats for 4 weeks, and hearing levels were measured via auditory brainstem response (ABR) tests. The qRT-PCR of miRNA ( $n = 8$ ), the predicted target genes ( $n = 8$  per group), and Western blotting ( $n = 6$ ) were conducted using cochlear nuclei of the noise-exposed and control rats. \* White noise (115 dB SPL) 3 h/day 3 times a week.

The threshold shifts were maintained in the noise-exposure group at 1 week, 2 weeks, 2 months, and 3 months after the noise exposure (all  $p < 0.05$ ) (Figure 2).

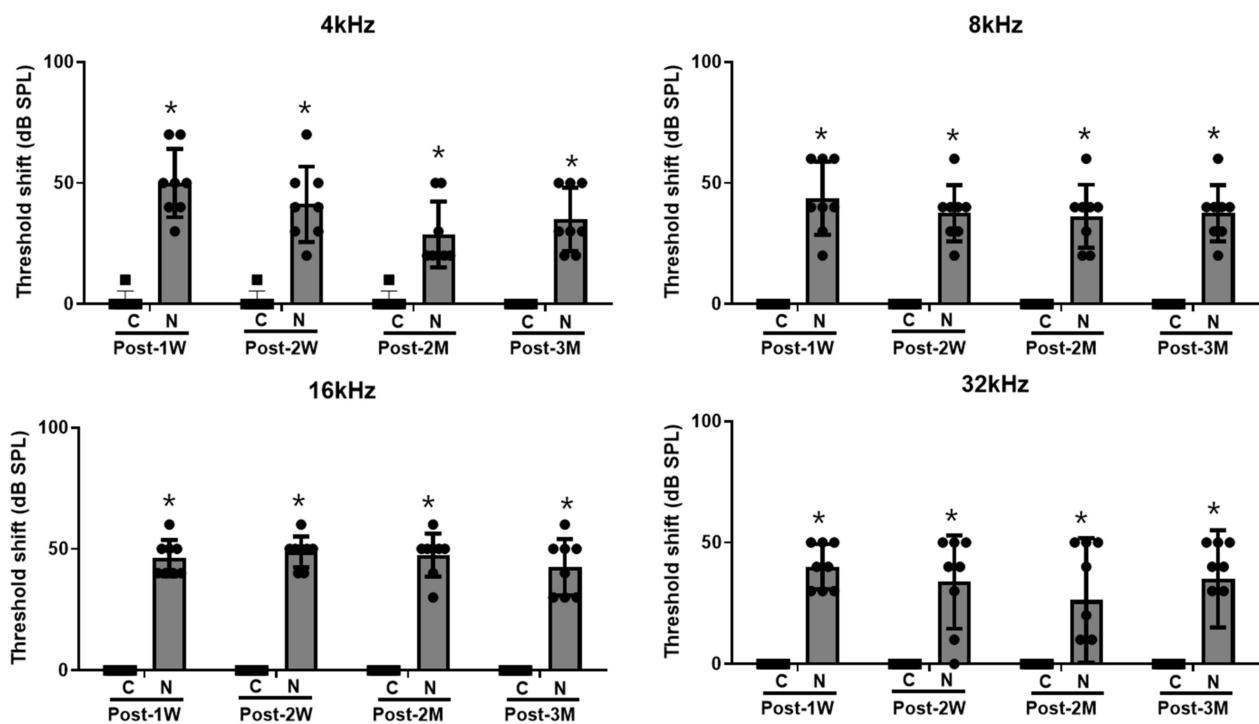


**Figure 2.** Hearing threshold shifts after noise exposure ( $n = 8$  per group). The noise exposed rats demonstrated hearing threshold shifts at 1 week, 2 weeks, 2 months, and 3 months post noise exposure at 4, 8, 16, and 32 kHz. (\*  $p < 0.05$ ; unpaired  $t$ -test between the control and noise-exposed groups; C: control rats; N: noise rats).

The protein expression levels of arc were higher in the CN of noise-exposed rats than in those of the control rats (0.95 [SD = 0.53] vs. 3.19 [SD = 1.00],  $p < 0.001$ ) (Figure 3). Brevican was also expressed at higher levels in the CN of noise-exposed rats than in those of the control rats (1.02 [SD = 0.10] vs. 1.66 [SD = 0.24],  $p < 0.001$ ) (Figure 3).

The expression levels of miR-758-5p, miR-15b-5p, miR-212-3p, miR-199a-5p, and miR-134-3p were lower in the noise-exposed rats than in the control rats (1.27 [SD = 0.37] vs. 0.04 [SD = 0.05],  $p < 0.001$  for miR-758-5p; 1.03 [SD = 0.54] vs. 0.24 [SD = 0.07],  $p < 0.001$  for miR-15b-5p; 1.15 [SD = 0.45] vs. 0.10 [SD = 0.04],  $p < 0.001$  for miR-212-3p; 0.92 [SD = 0.39] vs. 0.10 [SD = 0.05],  $p < 0.001$  for miR-199a-5p; 1.13 [SD = 0.54] vs. 0.07 [SD = 0.04],  $p < 0.001$  for miR-134-3p) (Figure 4).

Pathways involving miR-758-5p, miR-15b-5p, miR-212-3p, miR-199a-5p, and miR-134-3p were analyzed (Figure 5). FoxO signaling, dorsoventral axis formation, AMPK signaling, lysine degradation, focal adhesion, and PI3K-Akt signaling were found to be associated with these downregulated miRNAs.

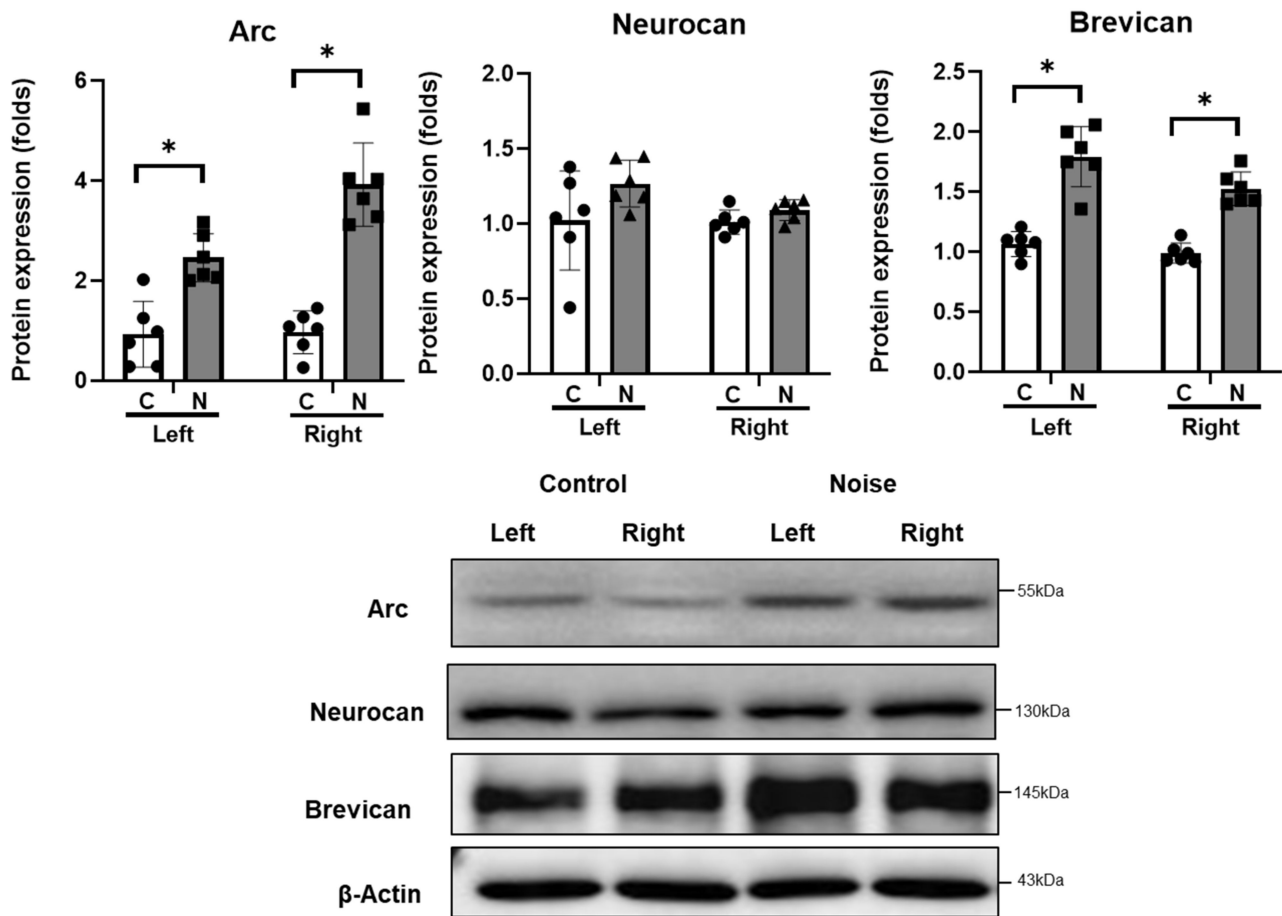


**Figure 3.** Arc, neurocan, and brevicin expression in the cochlear nuclei after noise exposure ( $n = 6$  per group). Arc and brevicin expression was increased in the noise-exposed group ( $* p < 0.05$ ; unpaired  $t$ -test between control and noise-exposed rats; C: control rats; N: noise rats).

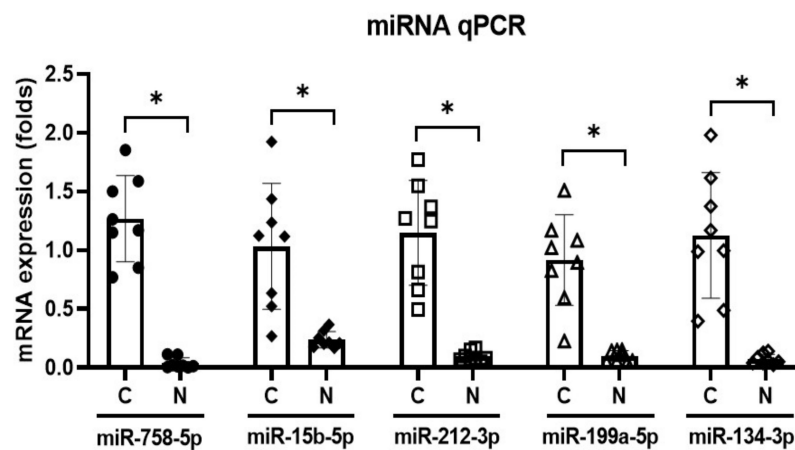


**Figure 4.** miR-758-5p, miR-15b-5p, miR-212-3p, miR-199a-5p, and miR-134-3p expression was reduced in the noise-exposed rats ( $n = 8$  per group;  $* p < 0.05$ ; unpaired  $t$ -test between control and noise-exposed rats).

KEGG pathway	p-value	Genes (n)	miRNAs
FoxO signaling pathway	0.000	36	5
Proteoglycans in cancer	0.000	36	5
Dorso-ventral axis formation	0.000	13	5
Pathways in cancer	0.000	72	5
AMPK signaling pathway	0.003	27	5
Lysine degradation	0.004	10	5
Focal adhesion	0.009	41	5
PI3K-Akt signaling pathway	0.014	56	5
Oocyte meiosis	0.019	22	5

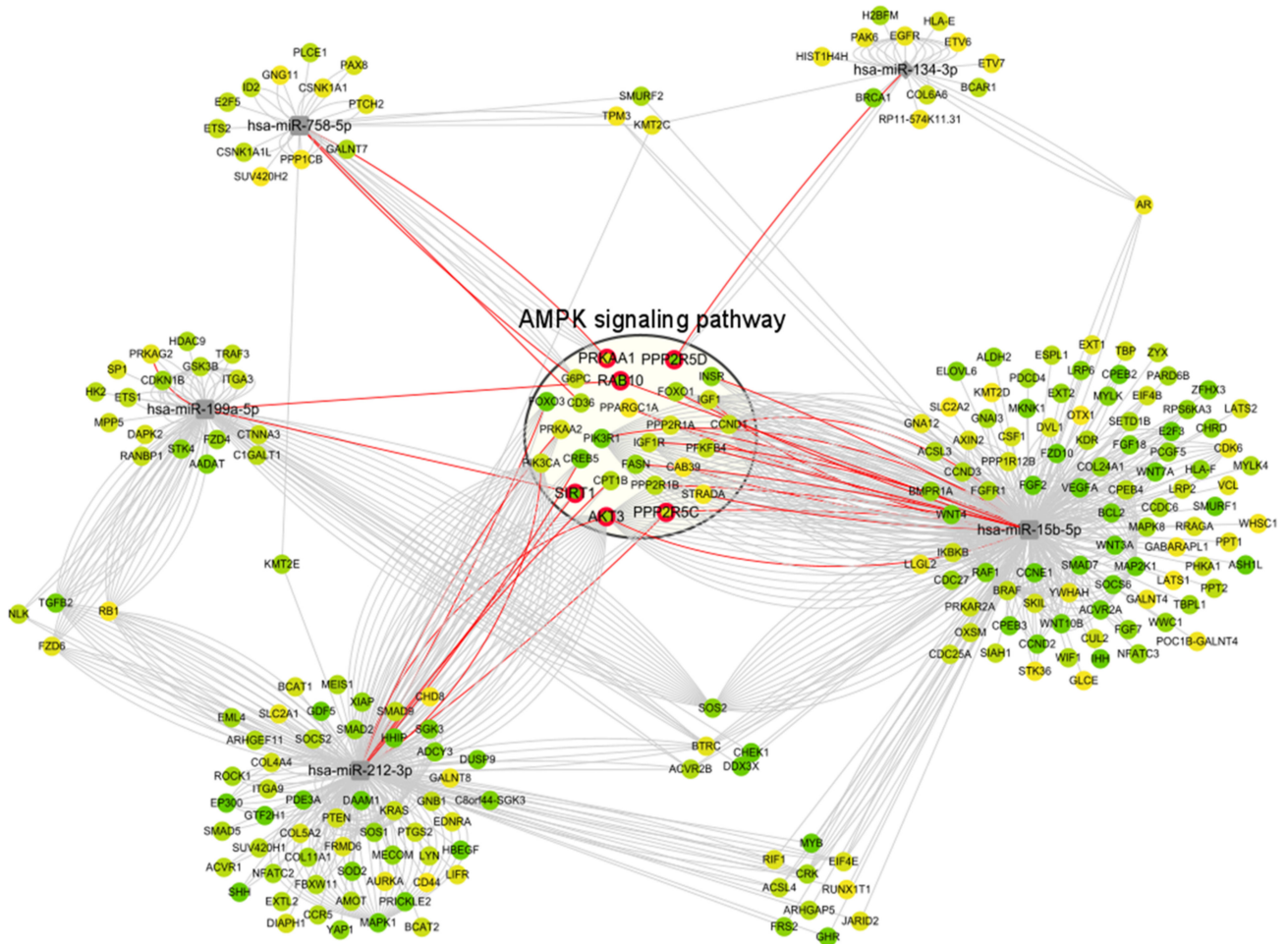


Figure 5. Pathways related to the dysregulated miRNAs in the cochlear nuclei of noise-exposed rats.

Among the predicted pathways, the AMPK signaling pathway was explored for related genes based on the previous studies which reported the modulation of AMPK signaling following noise-induced hearing loss [15,16]. Each miRNA was investigated for its associated target genes of the AMPK signaling pathway (Table 1). The predicted target genes of miR-758-5p-related AMPK signaling were *G6PC*, *PRKAA1*, and *SIRT1*. The predicted target genes of miR-15b-5p, i.e., *FASN*, *IGF1R*, *PPP2R5C*, *CCND1*, *PPP2R1A*, *PIK3R1*, *INSR*, and *IGF1*, were related to AMPK signaling. The predicted target genes of miR-212-3p, i.e., *PPP2R5C*, *AKT3*, *PIK3CA*, *FOXO3*, and *CPT1B*, were related to AMPK signaling. The predicted target genes of miR-199a-5p, i.e., *PRKAG2*, *RAB10*, *PRKAA2*, *SIRT1*, *CREB2*, and *PPP2R5C*, were involved in AMPK signaling. The predicted target gene of miR-134-3p was *PPP2R5D*.

**Table 1.** The predicted target genes related to the AMPK signaling pathway of the downregulated miRNAs in the cochlear nuclei of noise-exposed rats.

Related miRNA	Gene Name	Score	
hsa-miR-15b-5p	FASN	fatty acid synthase	0.935
	IGF1R	insulin like growth factor 1 receptor	0.866
	PPP2R5C	protein phosphatase 2 regulatory subunit B'gamma	0.845
	CCND1	cyclin D1	0.873
	PPP2R1A	protein phosphatase 2 scaffold subunit Aalpha	0.847
	PIK3R1	phosphoinositide-3-kinase regulatory subunit 1	0.989
	INSR	insulin receptor	0.947
	IGF1	insulin like growth factor 1	0.859
	AKT3	AKT serine/threonine kinase 3	1
	PPARGC1A	PPARG coactivator 1 alpha	0.806
	FOXO1	forkhead box O1	0.913
	CAB39	calcium binding protein 39	0.8
	PPP2R1B	protein phosphatase 2 scaffold subunit Abeta	0.885
	RAB10	RAB10, member RAS oncogene family	0.941
	PFKFB4	6-phosphofructo-2-kinase/fructose-2,6-biphosphatase 4	0.872
	STRADA	STE20 related adaptor alpha	0.81
	hsa-miR-758-5p	CD36	CD36 molecule
G6PC		glucose-6-phosphatase catalytic subunit 1	0.865
PRKAA1		protein kinase AMP-activated catalytic subunit alpha 1	0.84
hsa-miR-199a-5p	SIRT1	sirtuin 1	0.9
	PRKAG2	protein kinase AMP-activated non-catalytic subunit gamma 2	0.831
	RAB10	RAB10, member RAS oncogene family	0.954
	PRKAA2	protein kinase AMP-activated catalytic subunit alpha 2	0.844
hsa-miR-212-3p	SIRT1	sirtuin 1	1
	CREB5	cAMP responsive element binding protein 5	0.982
	PPP2R5C	protein phosphatase 2 regulatory subunit B'gamma	0.889
	AKT3	AKT serine/threonine kinase 3	0.92
	PIK3CA	phosphatidylinositol-4,5-bisphosphate 3-kinase catalytic subunit alpha	0.864
	FOXO3	forkhead box O3	0.997
	CPT1B	carnitine palmitoyltransferase 1B	0.892
hsa-miR-134-3p	PPP2R5D	protein phosphatase 2 regulatory subunit B'delta	0.965

Among the predicted genes related to AMPK signaling, *PPP2R5C*, *AKT3*, *RAB10*, *SIRT1*, *PRKAA1*, and *PPP2R5D* were examined for their mRNA expression levels using qRT-PCR (Figure 6). The mRNA expression levels of *AKT3*, *SIRT1*, and *PRKAA1* were higher in the noise-exposed rats than in the control rats (1.05 [SD = 0.38] vs. 1.76 [SD = 0.78],  $p = 0.039$  for *AKT3*; 1.00 [SD = 0.16] vs. 1.78 [SD = 0.76],  $p = 0.013$  for *SIRT1*; 1.01 [SD = 0.11] vs. 1.42 [SD = 0.17],  $p < 0.001$  for *PRKAA1*).

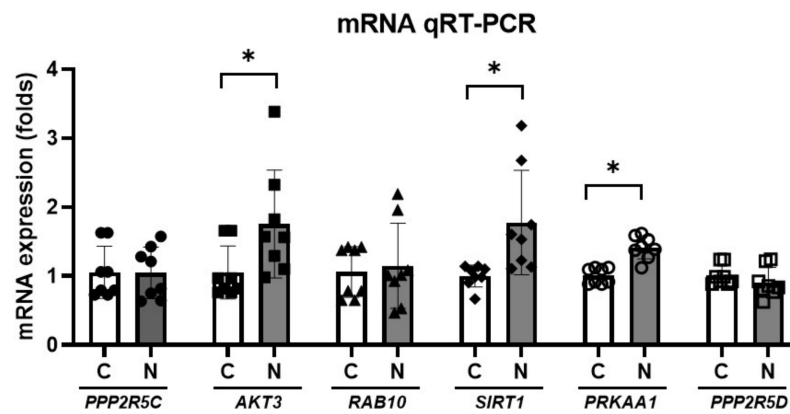


**Figure 6.** mRNA expression levels of *PPP2R5C*, *AKT3*, *RAB10*, *SIRT1*, *PRKAA1*, and *PPP2R5D* were higher in the noise-exposed rats than in the control rats ( $n = 8$  per group;  $* p < 0.05$ ; unpaired  $t$ -test between control and noise-exposed rats).

The protein expression level of *SIRT1* was higher in the noise-exposed rats than control rats (1.00 [SD = 0.17] vs. 1.50 [SD = 0.15],  $p < 0.001$ , Figure 7). The protein expression levels related with apoptosis were also higher in the noise-exposed rats than control rats (1.00 [SD = 0.16] vs. 1.55 [SD = 0.37],  $p = 0.013$  for caspase 3; 1.00 [SD = 0.33] vs. 1.53 [SD = 0.31],  $p = 0.016$  for cleaved caspase 3).

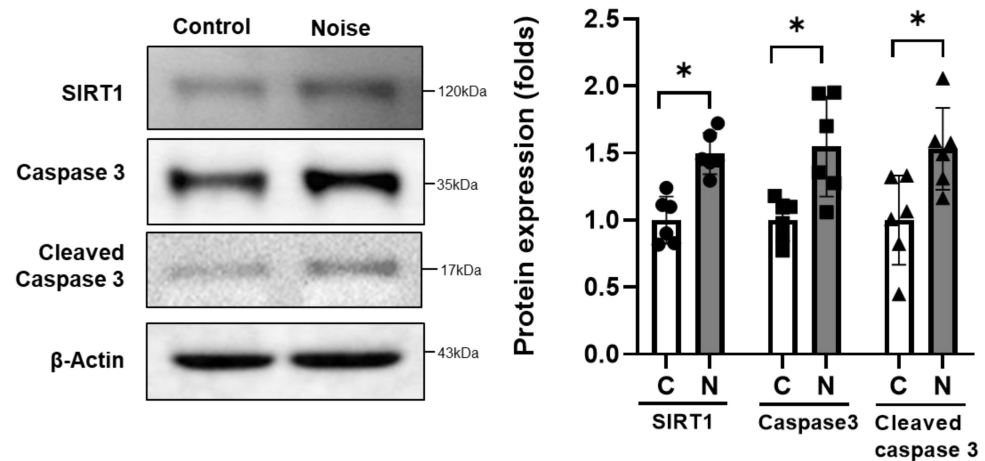


**Figure 7.** *SIRT1*, caspase 3, and cleaved caspase 3 expression in the cochlear nuclei after noise exposure ( $n = 6$  per group). *SIRT1*, caspase 3, and cleaved caspase 3 expressions were higher in the noise-exposed group ( $* p < 0.05$ ; unpaired  $t$ -test between control and noise-exposed rats; C: control rats; N: noise rats).

### 3. Discussion

In the present study, the CN of noise-exposed rats demonstrated an increased expression of brevicin. Five miRNAs, miR-758-5p, miR-15b-5p, miR-212-3p, miR-199a-5p, and miR-134-3p, were downregulated in the CN of noise-exposed rats. These downregulated miRNAs were related to the AMPK signaling pathway. Among the predicted target genes related to the AMPK signaling pathway, the mRNA expression of *AKT3* and *SIRT1* was increased in the CN of noise-exposed rats. These changes particularly in AMPK signaling pathway can be related with the increased expression of brevicin.

In this study, several miRNAs were found to be differentially expressed in CN following chronic noise exposure. A number of prior studies described the plausible mechanisms of these miRNAs with neural plastic changes [17–22]. miR-15b was reported to control epigenetics by inhibiting the methylation of cyclin D1 through the downregulation of a key enzyme (methylcytosine dioxygenase) in the ten-eleven translocation family, thereby

dysregulating the cell cycle and differentiation of neural progenitors and accelerating neurogenesis [17]. In patients with Alzheimer's disease, blood levels of miR-15b were downregulated compared to those in the control participants [18]. miR-212 has been characterized as a regulator of synaptic plasticity following external stimuli [19]. The dysregulation of miR-212, both overexpression and conditional knockout, induces anxiety-like behaviors following acute and chronic stress exposure [19]. In the animal models with dysregulated miR-212 expression, *SIRT1* and *AKT* were suggested to be involved as target genes of miR-212 [19]. In addition, the expression levels of miR-212 were reduced in neutrally derived plasma exosomes from patients with Alzheimer's disease [20]. miR-199a was suggested to inhibit neuritin in the hippocampus and cortex in the early stage of an Alzheimer's disease model (APP<sup>SWE</sup>, PSEN1<sup>dE9</sup> transgenic mice) [21]. miR-134 is mainly localized in the synapto-dendritic regions and is presumed to repress synaptic plasticity [10]. Following exposure to unpredictable chronic mild stress, miR-134 inhibits the phosphorylation of synapse-associated proteins of LIM-domain kinase 1 and cofilin, which reduces synaptic plasticity and induces depression-like behavior [22]. Thus, reduced miR-134 expression in the noise-exposed rats in the current study implied neural plastic changes induced by the noise stimulus.

The AMPK pathway involving *SIRT1* and *AKT* was suggested as a target pathway for the downregulated miRNAs of CN in noise-exposed rats in the current study. AMPK and *SIRT1* are evolutionarily similar proteins that share common target molecules to regulate metabolism and inflammation [23]. AMPK expression in the cochlear spiral ligament was transiently enhanced following noise exposure. AMPK is activated by pathological stresses such as hypoxia, oxidative stress, and noise exposure [16]. Upon the activation of AMPK, the expression of *SIRT1* increases and induces signaling cascades involving *AKT* [24].

In the present study, *SIRT1* expression was increased in the CN of noise-exposed rats. *SIRT1* is a homolog of sirtuins (*SIRT1*–*SIRT7*), which are predominantly expressed in the central nervous system [25]. As an oxidized nicotinamide adenine dinucleotide-dependent histone and nonhistone deacetylase, *SIRT1* responds to various external stimuli via deacetylation of several transcription factors associated with inflammation and apoptosis [26,27]. *SIRT1* has been suggested to be crucial to determine stress-induced anhedonia, as it enhances anxiety and depression [28]. Although the pathophysiological mechanism is still elusive, activation of *SIRT1* is supposed to reinforce signaling cascades, such as ERK1/2 cascades, and inhibit neurogenesis [28,29]. *SIRT1* activates *AKT* expression and promotes axonogenesis [30]. In animal models exposed to external stimuli, such as cerebral ischemia and exercise, *SIRT1* was upregulated with the activation of *AKT* signaling cascades and pro-apoptotic caspase 3 expression [24,31].

In this study, expression of *AKT3* was increased in the CN of noise-exposed rats. *AKT* was upregulated in selective nerve fibers of the osseous spiral lamina of the cochleae in noise-exposed guinea pigs [32]. *AKT* is activated by distress, including ischemia and noise exposure, and activates a number of survival pathways, including counteracting apoptosis [33,34]. As most cell types of the organ of Corti, stria vascularis, and supporting cells exhibited reduced expression of *AKT* following noise exposure, it was presumed that noise distress induced pro-apoptotic responses, and selective nerve fibers that showed increased *AKT* expression might be more responsive to noise stimuli, which led to early spatial activation of the antiapoptotic pathway [32]. Dysregulation of *AKT* signaling has been demonstrated in the cochleae of animals with noise-induced, aminoglycoside-induced, and aging-related hearing loss [35–38].

The expression of brevican is increased in the CN of noise-exposed rats of the present study. Although the molecular mechanisms underlying the changes in brevican expression in the CN are elusive, the elevated *AKT* levels could be associated with the increased expression of brevican in the CN of noise-exposed rats. Although the molecular mechanisms linking AMPK signaling involving *SIRT1* and *AKT* with CSPGs is still elusive, a prior study suggested the AMPK signaling induced regulation of CSPGs in brain tumor [39]. In addition, It has been reported to induce the expression of neurocan and brevican in astro-

cytes [40]. High levels of CSPGs, such as Neurocan and Brevican, inhibit axonal growth by inducing astrogliosis and glial scarring [41,42]. Thus, the high levels of AKT might be related to the high expression of brevican in this study. In addition, increased expression of brevican may induce glial scarring and inhibition of axonal regeneration in the CN following chronic noise exposure. Although the auditory threshold shifts were examined, the quantitative analyses on the cochleae cannot be conducted in this study due to the small number of study group. Because the noise exposure condition of the current study was enough to induce permanent threshold shifts, we can presume the cochlear dysfunction and injuries through all turns of cochleae. Further studies are needed to delineate the specific miRNAs inducing molecular cascades involving AKT and brevican in the CN following chronic noise exposure. Moreover, the clinical relevance of these molecular pathways in chronic noise-induced hearing loss condition without total deafness should be unraveled in follow-up research.

#### 4. Materials and Methods

##### 4.1. Noise and Comparison Groups

The Institutional Animal Care and Use Committee of CHA University Medical School (IACUC190046) approved this study. All experimental procedures followed the guidelines of the Institutional Animal Care and Use Committee of CHA University Medical School. The rats (postnatal eight-week Sprague-Dawley) were divided into control and noise-exposed groups (Figure 1). The rats in the noise-exposed group were exposed to wideband noise (2–20 kHz, 115 dB SPL, 4 h/day for 3 days/week for 4 weeks) in free-field condition using a speaker placed at the ceiling of the noise box (Tucker-Davis Technologies; Alachua, FL, USA). The 115 dB SPL of noise was applied to result in a permanent threshold shift. We chose the profound hearing loss animals to exclude the neural plasticity due to the recovery of hearing loss, which can be mixed up with the neural plasticity from the auditory deprivation. Rats were not anesthetized during noise exposure and the noise box was soundproofed. Rats in the control group were raised with ambient noise of approximately 40–60 dB SPL. Hearing levels were estimated using auditory brainstem response (ABR) thresholds. Two months after noise exposure, all rats were euthanized and the cochleae and CN were dissected [43].

##### 4.2. Hearing Level Measurement

Hearing levels were measured using SmartEP Intelligent Hearing System (Miami, FL, USA) [44]. ABR measurements were conducted under anesthesia (40 mg/kg zoletil and 10 mg/kg xylazine). The reference, ground, and measuring electrodes were placed in the vertex, contralateral thigh, and ipsilateral retroauricular space, respectively. A plastic earphone was placed into the ipsilateral ear canal and connected to an EC1 electrostatic speaker. Pure tone sound stimuli were delivered to earphones at frequencies of 4, 8, 16, and 32 kHz (duration: 1562  $\mu$ s; envelope: Blackman; stimulation rate: 21.1/s; amplitude: 90–20 dB SPL, 1024 sweeps). The hearing threshold was set as the lowest sound amplitude-evoked wave II [45].

##### 4.3. Protein Expression in CN

The expression levels of arc, neurocan, brevican, SIRT1, caspase 3, and cleaved caspase 3 were evaluated in the CN. The protein was purified from CN tissue using a lysis buffer (Pre-prep, Intron). Equal amounts of protein samples were subjected to 8–10% sodium dodecyl sulfate-polyacrylamide gel electrophoresis. After transferring the resolved proteins onto polyvinylidene difluoride membranes (Merck Millipore, Burlington, MA, USA), they were incubated with 1:1000 anti-arc (Santa Cruz, Dallas, TX, USA, sc166461), anti-neurocan (Mybiosource, San Diego, CA, USA, MBS822310), anti-brevican (Santa Cruz, Dallas, TX, USA, sc135849), anti-SIRT1 (Santa Cruz, Dallas, TX, USA, sc74465), caspase 3 (Cell Signaling Technology, 9662s), cleaved caspase 3 (Cell Signaling Technology, Danvers, MA, USA, 9661s), and anti-rabbit monoclonal  $\beta$ -actin antibodies (Cell Signaling Technology, D6A8). Horseradish peroxidase (HRP)-conjugated secondary antibodies were treated with 1:2000

anti-rabbit IgG, HRP-linked (Cell Signaling Technology, 7074s), and goat anti-mouse IgG H&L (HRP) (Abcam, Cambridge, England, ab97023). The membranes were visualized using an enhanced chemiluminescence kit (Bio-Rad, Hercules, CA, USA). Protein bands were quantified using the ImageJ software (National Institutes of Health, Bethesda, MD, USA).

#### 4.4. miRNA Expression in the CN

The miRNAs that showed expression changes following noise exposure or hearing loss in the central nervous system were examined in the CN of rats exposed to chronic noise. CN from eight rats per group were analyzed. MDNA was synthesized from purified miRNAs using the miScript<sup>®</sup> II RT kit (Qiagen, Hilden, Germany). PCR was conducted using the miScript SYBR<sup>®</sup> Green PCR kit (Qiagen) with the miScript Primer Assay reagents (Qiagen). U6 small nuclear RNA was used as the reference. ABI 7500 real-time PCR system (Applied Biosystems, Foster City, CA, USA) was used. The expression levels of miRNAs were quantified using cycle threshold (Ct) values and the  $2^{-\Delta\Delta C_t}$  method.

#### 4.5. The Predicted Target Genes for miRNAs

The predicted target pathways and related genes for the dysregulated miRNAs were accessed using DIANA-mirPath v.3 (Available online: <http://snf-515788.vm.okeanos.grnet.gr/> (accessed on 7 June 2021)). KEGG pathways and the related target genes were searched with a threshold of 0.8 and a false discovery rate correction [46].

The mRNA expression of the predicted target genes was analyzed using quantitative reverse-transcription-PCR (qRT-PCR) [47,48]. Following reverse transcription of cDNA from purified RNA, the reagent was prepared using TOPreal<sup>™</sup> qPCR 2× PreMIX (SYBR Green with low ROX; Enzymomics; Daejeon, Korea). PCR was conducted using the ViiA7 real-time PCR system (Applied Biosystems, Carlsbad, CA, USA). The primer sets used in this study are listed in Table 2. Glyceraldehyde 3-phosphate dehydrogenase (*GAPDH*) was used as the reference gene. mRNA expression levels were quantified using the  $2^{-\Delta\Delta C_t}$  method.

**Table 2.** Oligonucleotide primer sequences for quantitative reverse transcriptase polymerase chain reaction.

Gene	Primer Sequence (Forward)	Primer Sequence (Reverse)	Annealing Temperature (°C)	Product Size (bp)
<i>PPP2R5C</i>	5'-CTAGCCAAAGCGAATCCCA-3'	5'-GAGTCTCGTCGCTCACTGTC-3'	60	93
<i>AKT3</i>	5'-CCACCTGAAAAGTATGACGACG-3'	5'-TAAGAGCGAGGACTGGTGGA-3'	60	133
<i>RAB10</i>	5'-TTGTTTGCCCCACTACTCC-3'	5'-TAAATGAGGGGCTGACACCG-3'	60	185
<i>SIRT1</i>	5'-GCAGGTTGCGGGAATCCAA-3'	5'-GGCAAGATGCTGTTCGAAA-3'	60	155
<i>PRKAA1</i>	5'-GGGTGAAGATCGGCCACTAC-3'	5'-CTCTCTGCGGATTTCCCGA-3'	60	62
<i>PPP2R5D</i>	5'-CGAGTCGGGTCGCTAAGAAG-3'	5'-ACACTCAGAGTCAAAGGCG-3'	60	164
<i>GAPDH</i>	5'-AGTGCCAGCCTCGTCTCATA-3'	5'-AAGAGAAGGCAGCCCTGGTA-3'	60	93

#### 4.6. Statistical Analysis

The hearing threshold shifts after the noise exposure were compared between noise-exposed and control rats using an unpaired *t*-test. The mRNA and miRNA expression levels in noise-exposed and control rats were compared using the unpaired *t*-test. The results are presented as mean ± standard deviation (SD). All analyses were conducted using the SPSS software (ver. 21.0; IBM Corp.; Armonk, NY, USA). Statistical significance was set at  $p \leq 0.05$ .

## 5. Conclusions

The CN of noise-exposed rats exhibited elevated expression of arc and brevicin. The levels of several miRNAs, including miR-758-5p, miR-15b-5p, miR-212-3p, miR-199a-5p, and miR-134-3p, were low in the CN of rats exposed to chronic noise. The AMPK signaling pathway involving *AKT3* and *SIRT1* was predicted to be activated in noise-exposed rats.

**Author Contributions:** Conceptualization, S.Y.K.; methodology, S.Y.K.; formal analysis, S.Y.K., J.J. and S.M.L.; writing—original draft preparation, S.Y.K.; writing—review and editing, S.Y.K., C.H.L. and S.M.L.; funding acquisition, S.Y.K. and C.H.L. All authors have read and agreed to the published version of the manuscript.

**Funding:** This research was supported by funding from the National Research Foundation (NRF) of Korea (2020R1A2C4002594 (Approval date: 1 March 2020)) and a grant of the Research Driven Hospital R&D project, funded by the CHA Bundang Medical Center (grant number: BDCHA R&D 2021-003) The APC was funded by BDCHA R&D 2021-003.

**Institutional Review Board Statement:** The Institutional Animal Care and Use Committee of CHA University (IACUC190046) approved the performed animal experiments. The conditions of animal rearing, drug administration, and sacrifice complied with the regulations of the Institutional Animal Care and Use Committee of CHA University.

**Informed Consent Statement:** Not applicable.

**Data Availability Statement:** The data presented in this study are available upon request from the corresponding author.

**Conflicts of Interest:** The authors declare no conflict of interest. The funders had no role in the design of the study; in the collection, analyses, or interpretation of data; in the writing of the manuscript; or in the decision to publish the results.

## References

- Manohar, S.; Ramchander, P.; Salvi, R.; Seigel, G. Synaptic Reorganization Response in the Cochlear Nucleus Following Intense Noise Exposure. *Neuroscience* **2018**, *399*, 184–198. [[CrossRef](#)] [[PubMed](#)]
- Manley, G.A. The mammalian Cretaceous cochlear revolution. *Hear. Res.* **2017**, *352*, 23–29. [[CrossRef](#)] [[PubMed](#)]
- Weinrich, L.; Sonntag, M.; Arendt, T.; Morawski, M. Neuroanatomical characterization of perineuronal net components in the human cochlear nucleus and superior olivary complex. *Hear. Res.* **2018**, *367*, 32–47. [[CrossRef](#)]
- Favuzzi, E.; Marques-Smith, A.; Deogracias, R.; Winterflood, C.M.; Sánchez-Aguilera, A.; Mantoan, L.; Maeso, P.; Fernandes, C.; Ewers, H.; Rico, B. Activity-Dependent Gating of Parvalbumin Interneuron Function by the Perineuronal Net Protein Brevican. *Neuron* **2017**, *95*, 639–655.e10. [[CrossRef](#)]
- Nguyen, A.; Khaleel, H.M.; Razak, K.A. Effects of noise-induced hearing loss on parvalbumin and perineuronal net expression in the mouse primary auditory cortex. *Hear. Res.* **2017**, *350*, 82–90. [[CrossRef](#)]
- Park, S.S.; Lee, D.H.; Lee, S.M.; Lee, C.H.; Kim, S.Y. Noise exposure alters MMP9 and brevicin expression in the rat primary auditory cortex. *BMC Neurosci.* **2020**, *21*, 16. [[CrossRef](#)] [[PubMed](#)]
- Krohs, C.; Bordeynik-Cohen, M.; Messika-Gold, N.; Elkon, R.; Avraham, K.B.; Nothwang, H.G. Expression pattern of cochlear microRNAs in the mammalian auditory hindbrain. *Cell Tissue Res.* **2021**, *383*, 655–666. [[CrossRef](#)] [[PubMed](#)]
- Park, S.; Han, S.H.; Kim, B.G.; Suh, M.W.; Lee, J.H.; Oh, S.H.; Park, M.K. Changes in microRNA Expression in the Cochlear Nucleus and Inferior Colliculus after Acute Noise-Induced Hearing Loss. *Int. J. Mol. Sci.* **2020**, *21*, 8792. [[CrossRef](#)]
- Giraldez, A.J.; Cinalli, R.M.; Glasner, M.E.; Enright, A.; Thomson, J.M.; Baskerville, S.; Hammond, S.M.; Bartel, D.P.; Schier, A.F. MicroRNAs Regulate Brain Morphogenesis in Zebrafish. *Science* **2005**, *308*, 833–838. [[CrossRef](#)] [[PubMed](#)]
- Schratt, G.M.; Tuebing, F.; Nigh, E.A.; Kane, C.G.; Sabatini, M.E.; Kiebler, M.; Greenberg, M.E. A brain-specific microRNA regulates dendritic spine development. *Nature* **2006**, *439*, 283–289. [[CrossRef](#)]
- Higuchi, F.; Uchida, S.; Yamagata, H.; Abe-Higuchi, N.; Hobara, T.; Hara, K.; Kobayashi, A.; Shintaku, T.; Itoh, Y.; Suzuki, T.; et al. Hippocampal MicroRNA-124 Enhances Chronic Stress Resilience in Mice. *J. Neurosci.* **2016**, *36*, 7253–7267. [[CrossRef](#)] [[PubMed](#)]
- Schlüter, T.; Berger, C.; Rosengauer, E.; Fieth, P.; Krohs, C.; Ushakov, K.; Steel, K.P.; Avraham, K.B.; Hartmann, A.K.; Felmy, F.; et al. miR-96 is required for normal development of the auditory hindbrain. *Hum. Mol. Genet.* **2018**, *27*, 860–874. [[CrossRef](#)] [[PubMed](#)]
- Friedman, L.M.; Dror, A.A.; Mor, E.; Tenne, T.; Toren, G.; Satoh, T.; Biesemeier, D.J.; Shomron, N.; Fekete, D.M.; Hornstein, E.; et al. MicroRNAs are essential for development and function of inner ear hair cells in vertebrates. *Proc. Natl. Acad. Sci. USA* **2009**, *106*, 7915–7920. [[CrossRef](#)] [[PubMed](#)]
- Napoli, D.; Lupori, L.; Mazziotti, R.; Sagona, G.; Bagnoli, S.; Samad, M.; Sacramento, E.K.; Kirkpartick, J.; Putignano, E.; Chen, S.; et al. MiR-29 coordinates age-dependent plasticity brakes in the adult visual cortex. *EMBO Rep.* **2020**, *21*, e50431. [[CrossRef](#)] [[PubMed](#)]
- Hill, K.; Yuan, H.; Wang, X.; Sha, S.H. Noise-Induced Loss of Hair Cells and Cochlear Synaptopathy Are Mediated by the Activation of AMPK. *J. Neurosci.* **2016**, *36*, 7497–7510. [[CrossRef](#)] [[PubMed](#)]
- Nagashima, R.; Yamaguchi, T.; Kuramoto, N.; Ogita, K. Acoustic overstimulation activates 5'-AMP-activated protein kinase through a temporary decrease in ATP level in the cochlear spiral ligament prior to permanent hearing loss in mice. *Neurochem. Int.* **2011**, *59*, 812–820. [[CrossRef](#)]
- Noack, F.; Calegari, F. Micro- RNA s meet epigenetics to make for better brains. *EMBO Rep.* **2014**, *15*, 1224–1225. [[CrossRef](#)]

18. Wu, H.Z.Y.; Thalamuthu, A.; Cheng, L.; Fowler, C.; Masters, C.L.; Sachdev, P.; Mather, K.A. Differential blood miRNA expression in brain amyloid imaging-defined Alzheimer's disease and controls. *Alzheimers Res. Ther.* **2020**, *12*, 59. [[CrossRef](#)]
19. Aten, S.; Page, C.E.; Kalidindi, A.; Wheaton, K.; Niraula, A.; Godbout, J.P.; Hoyt, K.; Obrietan, K. miR-132/212 is induced by stress and its dysregulation triggers anxiety-related behavior. *Neuropharmacology* **2018**, *144*, 256–270. [[CrossRef](#)]
20. Cha, D.J.; Mengel, D.; Mustapic, M.; Liu, W.; Selkoe, D.J.; Kapogiannis, D.; Galasko, D.; Rissman, R.A.; Bennett, D.A.; Walsh, D.M. miR-212 and miR-132 Are Downregulated in Neurally Derived Plasma Exosomes of Alzheimer's Patients. *Front. Neurosci.* **2019**, *13*, 1208. [[CrossRef](#)]
21. Song, D.; Li, G.; Hong, Y.; Zhang, P.; Zhu, J.; Yang, L.; Huang, J. miR-199a decreases Neuritin expression involved in the development of Alzheimer's disease in APP/PS1 mice. *Int. J. Mol. Med.* **2020**, *46*, 384–396. [[CrossRef](#)] [[PubMed](#)]
22. Fan, C.; Zhu, X.; Song, Q.; Wang, P.; Liu, Z.; Yu, S.Y. MiR-134 modulates chronic stress-induced structural plasticity and depression-like behaviors via downregulation of Limk1/cofilin signaling in rats. *Neuropharmacology* **2018**, *131*, 364–376. [[CrossRef](#)] [[PubMed](#)]
23. Ruderman, N.B.; Xu, X.J.; Nelson, L.; Cacicedo, J.M.; Saha, A.K.; Lan, F.; Ido, Y. AMPK and SIRT1: A long-standing partnership? *Am. J. Physiol. Endocrinol. Metab.* **2010**, *298*, E751–E760. [[CrossRef](#)]
24. Lin, J.Y.; Kuo, W.W.; Baskaran, R.; Kuo, C.H.; Chen, Y.A.; Chen, W.S.; Ho, T.J.; Day, C.H.; Mahalakshmi, B.; Huang, C.Y. Swimming exercise stimulates IGF1/PI3K/Akt and AMPK/SIRT1/PGC1 $\alpha$  survival signaling to suppress apoptosis and inflammation in aging hippocampus. *Aging* **2020**, *12*, 6852–6864. [[CrossRef](#)]
25. Ramadori, G.; Lee, C.E.; Bookout, A.L.; Lee, S.; Williams, K.; Anderson, J.; Elmquist, J.K.; Coppari, R. Brain SIRT1: Anatomical Distribution and Regulation by Energy Availability. *J. Neurosci.* **2008**, *28*, 9989–9996. [[CrossRef](#)]
26. Vaziri, H.; Dessain, S.K.; Eaton, E.N.; Imai, S.-I.; Frye, R.A.; Pandita, T.K.; Guarente, L.; Weinberg, R.A. hSIR2/SIRT1 Functions as an NAD-Dependent p53 Deacetylase. *Cell* **2001**, *107*, 149–159. [[CrossRef](#)]
27. Jeong, H.; Cohen, D.E.; Cui, L.; Supinski, A.; Savas, J.N.; Mazzulli, J.R.; Yates, J.R.; Bordone, L.; Guarente, L.; Krainc, D. Sirt1 mediates neuroprotection from mutant huntingtin by activation of the TORC1 and CREB transcriptional pathway. *Nat. Med.* **2011**, *18*, 159–165. [[CrossRef](#)] [[PubMed](#)]
28. Ferland, C.L.; Hawley, W.R.; Puckett, R.E.; Wineberg, K.; Lubin, F.D.; Dohanich, G.P.; Schrader, L.A. Sirtuin Activity in Dentate Gyrus Contributes to Chronic Stress-Induced Behavior and Extracellular Signal-Regulated Protein Kinases 1 and 2 Cascade Changes in the Hippocampus. *Biol. Psychiatry* **2013**, *74*, 927–935. [[CrossRef](#)]
29. Prozorovski, T.; Schulze-Toppf, U.; Glumm, R.; Baumgart, J.; Schröter, F.; Ninnemann, O.; Siegert, E.; Bendix, I.; Brüstle, O.; Nitsch, R.; et al. Sirt1 contributes critically to the redox-dependent fate of neural progenitors. *Nat. Cell Biol.* **2008**, *10*, 385–394. [[CrossRef](#)]
30. Li, X.H.; Chen, C.; Tu, Y.; Sun, H.T.; Zhao, M.L.; Cheng, S.X.; Qu, Y.; Zhang, S. Sirt1 Promotes Axonogenesis by Deacetylation of Akt and Inactivation of GSK3. *Mol. Neurobiol.* **2013**, *48*, 490–499. [[CrossRef](#)]
31. Teertam, S.K.; Babu, P.P. Differential role of SIRT1/MAPK pathway during cerebral ischemia in rats and humans. *Sci. Rep.* **2021**, *11*, 6339. [[CrossRef](#)] [[PubMed](#)]
32. Selivanova, O.; Brieger, J.; Heinrich, U.-R.; Mann, W. Akt and c-Jun N-terminal kinase are regulated in response to moderate noise exposure in the cochlea of guinea pigs. *ORL J. Otorhinolaryngol. Relat. Spec.* **2007**, *69*, 277–282. [[CrossRef](#)] [[PubMed](#)]
33. Plas, D.R.; Thompson, C.B. Akt-dependent transformation: There is more to growth than just surviving. *Oncogene* **2005**, *24*, 7435–7442. [[CrossRef](#)]
34. Duan, J.; Cui, J.; Zheng, H.; Xi, M.; Guo, C.; Weng, Y.; Yin, Y.; Wei, G.; Cao, J.; Wang, Y.; et al. *Aralia taibaiensis* Protects against I/R-Induced Brain Cell Injury through the Akt/SIRT1/FOXO3a Pathway. *Oxidative Med. Cell. Longev.* **2019**, *2019*, 7609765. [[CrossRef](#)] [[PubMed](#)]
35. Chen, J.; Yuan, H.; Talaska, A.E.; Hill, K.; Sha, S.-H. Increased Sensitivity to Noise-Induced Hearing Loss by Blockade of Endogenous PI3K/Akt Signaling. *J. Assoc. Res. Otolaryngol.* **2015**, *16*, 347–356. [[CrossRef](#)] [[PubMed](#)]
36. Sha, S.-H.; Chen, F.-Q.; Schacht, J. PTEN attenuates PIP3/Akt signaling in the cochlea of the aging CBA/J mouse. *Hear. Res.* **2010**, *264*, 86–92. [[CrossRef](#)] [[PubMed](#)]
37. Chung, W.-H.; Pak, K.; Lin, B.; Webster, N.; Ryan, A.F. A PI3K Pathway Mediates Hair Cell Survival and Opposes Gentamicin Toxicity in Neonatal Rat Organ of Corti. *J. Assoc. Res. Otolaryngol.* **2006**, *7*, 373–382. [[CrossRef](#)]
38. Lai, R.; Li, W.; Hu, P.; Xie, D.; Wen, J. Role of Hsp90/Akt pathway in the pathogenesis of gentamicin-induced hearing loss. *Int. J. Clin. Exp. Pathol.* **2018**, *11*, 4431–4438.
39. Kim, Y.; Kang, H.; Powathil, G.; Kim, H.; Trucu, D.; Lee, W.; Lawler, S.; Chaplain, M. Role of extracellular matrix and microenvironment in regulation of tumor growth and LAR-mediated invasion in glioblastoma. *PLoS ONE* **2018**, *13*, e0204865. [[CrossRef](#)]
40. Jahan, N.; Hannila, S.S. Transforming growth factor  $\beta$ -induced expression of chondroitin sulfate proteoglycans is mediated through non-Smad signaling pathways. *Exp. Neurol.* **2015**, *263*, 372–384. [[CrossRef](#)]
41. Silver, J.; Miller, J.H. Regeneration beyond the glial scar. *Nat. Rev. Neurosci.* **2004**, *5*, 146–156. [[CrossRef](#)] [[PubMed](#)]
42. Bradbury, E.J.; Moon, L.; Popat, R.J.; King, V.R.; Bennett, G.S.; Patel, P.N.; Fawcett, J.; McMahon, S. Chondroitinase ABC promotes functional recovery after spinal cord injury. *Nature* **2002**, *416*, 636–640. [[CrossRef](#)] [[PubMed](#)]
43. Han, K.H.; Cho, H.; Han, K.R.; Mun, S.K.; Kim, Y.K.; Park, I.; Chang, M. Role of microRNA-375-3p-mediated regulation in tinnitus development. *Int. J. Mol. Med.* **2021**, *48*, 136. [[CrossRef](#)] [[PubMed](#)]

44. Kim, S.Y.; Heo, H.; Kim, D.H.; Kim, H.J.; Oh, S.H. Neural Plastic Changes in the Subcortical Auditory Neural Pathway after Single-Sided Deafness in Adult Mice: A MEMRI Study. *BioMed Res. Int.* **2018**, *2018*, 8624745. [[CrossRef](#)] [[PubMed](#)]
45. Alvarado, J.C.; Fuentes-Santamaría, V.; Jareño-Flores, T.; Blanco, J.L.; Juiz, J.M. Normal variations in the morphology of auditory brainstem response (ABR) waveforms: A study in wistar rats. *Neurosci. Res.* **2012**, *73*, 302–311. [[CrossRef](#)]
46. Vlachos, I.S.; Zagganas, K.; Paraskevopoulou, M.D.; Georgakilas, G.; Karagkouni, D.; Vergoulis, T.; Dalamagas, T.; Hatzigeorgiou, A.G. DIANA-miRPath v3.0: Deciphering microRNA function with experimental support. *Nucleic Acids Res.* **2015**, *43*, W460–W466. [[CrossRef](#)] [[PubMed](#)]
47. Kim, S.Y.; Kim, J.K.; Park, S.H.; Kim, B.G.; Jang, A.S.; Oh, S.H.; Lee, J.H.; Suh, M.W.; Park, M.K. Effects of inhaled particulate matter on the central nervous system in mice. *NeuroToxicology* **2018**, *67*, 169–177. [[CrossRef](#)]
48. Bustin, S.A.; Benes, V.; Garson, J.A.; Hellemans, J.; Huggett, J.; Kubista, M.; Mueller, R.; Nolan, T.; Pfaffl, M.W.; Shipley, G.L.; et al. The MIQE Guidelines: Minimum Information for Publication of Quantitative Real-Time PCR Experiments. *Clin. Chem.* **2009**, *55*, 611–622. [[CrossRef](#)]